Pathway Dependent Post-Assembly Modification of an Anthracene-Edged $M^{II}_4L_6$ Tetrahedron

Tanya K. Ronson, Ben S. Pilgrim and Jonathan R. Nitschke*

Department of Chemistry, University of Cambridge, Lensfield Road, Cambridge, CB2 1EW, UK

Supporting Information Placeholder

ABSTRACT: $Fe^{II}_4L_6$ tetrahedral cage **1** undergoes post-assembly modification (PAM) via a Diels-Alder cycloaddition of the anthracene panels of the cage with tetracyanoethylene. The modified cage **2** possesses an enclosed cavity suitable for encapsulation of the fullerene C_{60} whereas original cage **1** forms a unique covalent adduct through a Diels-Alder cycloaddition of three of its anthracene ligands with C_{60}. This adduct undergoes further PAM via reaction of the remaining three ligands with tetracyanoethylene, enabling the isolation of two distinct products depending on the order of addition of C_{60} and tetracyanoethylene. The modified cage **2** was also able to bind an anionic guest, $[Co(C_2B_9H_{11})_2]^-$, which was not encapsulated by the original cage, demonstrating the potential of PAM for tuning the binding properties of supramolecular hosts.

Post-assembly modification (PAM) of discrete supramolecular complexes has recently attracted increasing attention as a means of introducing new functionality[1], tuning solubility,[2] trapping species out of equilibrium[3] and constructing interlocked structures[4] and polymers.[5] PAM reactions should proceed quantitatively under mild conditions that do not disrupt the dynamic linkages that hold supramolecular structures together.[3] Although several reaction types, including olefin metathesis,[6] alkyne–azide cycloaddition,[7] imine reduction,[8] Diels-Alder cycloaddition (both normal[9] and inverse[10] electron-demand), Knoevenagel condensation,[11] acylation[3] and nucleophile-isocyanate coupling[9,12] have been employed to modify supramolecular species, solution-based PAM remains less explored than the PAM of more robust metal–organic frameworks.[13] In order to produce new functionalized supramolecular assemblies[14] for recognition,[15] catalysis,[16] sensing[8] and drug delivery,[17] it is crucial to expand the range of reaction types that can be employed for PAM.

Anthracene is an attractive moiety for incorporation into supramolecular hosts,[18] due to its extended π-surface, which may form favorable aromatic interactions with targeted guests, and its panel-like shape, which facilitates effective cavity enclosure and stronger host–guest interactions.[19] Although anthracene has been used as a structural element in metal-organic cages,[19] it has not yet been employed as a reactive element in discrete supramolecular constructs despite its well-known ability to undergo both thermal and photochemical cycloadditions across the 9 and 10 positions with a variety of partners.[20] It has found recent use as a structurally-modifiable element of the more robust covalent cyclophane-[21] and cycloparaphenylene-based[22] hosts, and also as a reagent employed to tether redox functionality onto maleimide-functionalized hexagonal prisms.[9]

Here we show how a new anthracene-edged $Fe^{II}_4L_6$ cage **1** undergoes PAM via Diels-Alder reaction with tetracyanoethylene (TCNE) under mild conditions (Scheme 1), and how the resultant conversion from planar anthracene to bent dihydroanthracene panels significantly influences the host-guest properties of the assembly. Remarkably, three of the six anthracene panels of **1** were also observed to undergo regiospecific Diels-Alder reactions with a single C_{60} to form a unique covalently-trapped adduct; the remaining three anthracene panels of this adduct then underwent further PAM with TCNE. The $Fe^{II}_4L_6$ cage is thus converted to two distinct post-assembly modified products depending on the order of reaction with C_{60} and TCNE (Scheme 2). These topologically complex modifications would be impossible to achieve if the isolated components of the system reacted together prior to assembly. The PAM strategy is also crucial due to functional group incompatibilities between the reaction components, as the free diamine precursor undergoes aza-Michael addition with TCNE.

Scheme 1. Self-assembly of anthracene-edged cage 1, and subsequent PAM by reaction with TCNE.

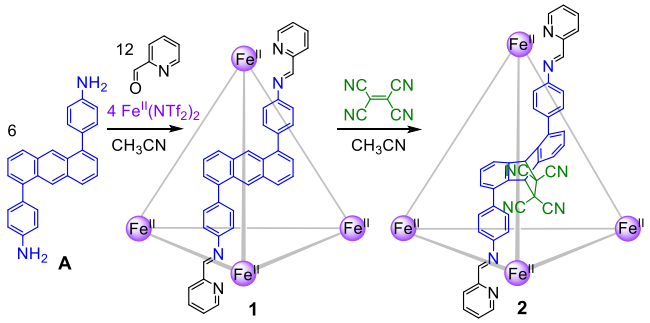

Anthracene-containing subcomponent **A** was synthesized in a single step from commercially available starting materials via a Pd-catalyzed Suzuki-Miyaura cross-coupling[23], as described in the Supporting Information. Cage **1** was then prepared via subcomponent self-assembly[24] of diamine **A** (6 equiv) with 2-formylpyridine (12 equiv) and iron(II) bis(trifluoromethane)sulfonimide ($Fe(NTf_2)_2$, 4 equiv). Electrospray ionization mass spectrometry (ESI-MS) confirmed the $Fe^{II}_4L_6$ stoichiometry of **1** (Figure S9). The ^1H and ^{13}C NMR spectra of cage **1** display a single set of ligand resonances in solution, consistent with idealized *T* point symmetry (Figures S3 and S4).

Scheme 2. Summary of the distinct pathways of PAM involving cage 1 to give [C_{60} ⊂ 2] or [C_{60} • 3], and the one-pot formation of [C_{60} ⊂ 2]. [a]

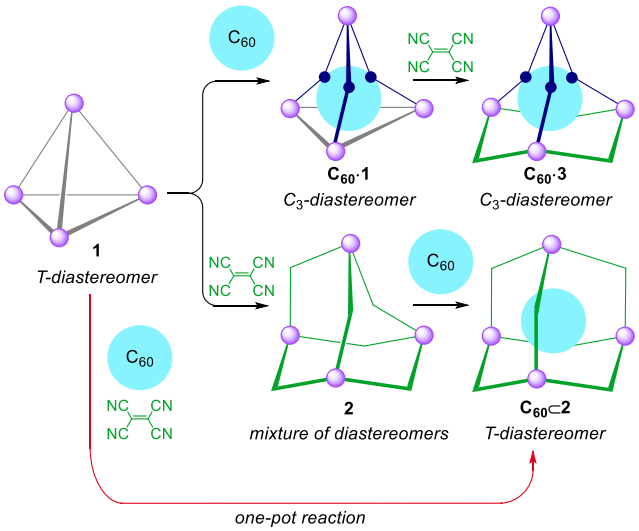

[a]Anthracene-based ligands are represented by straight lines and modified dihydroanthracene-based ligands by bent lines. Dark blue circles indicate covalent connection to C_{60}.

Single-crystal X-ray diffraction analysis (Figure 1) confirmed the tetrahedral structure of **1** in the solid state. Six *bis*-bidentate pyridylimine ligands bridge four facially coordinated Fe^{II} centers, resulting in a tetrahedral arrangement with approximate *T*-symmetry. All Fe^{II} stereocenters within a cage share the same *Δ* or *Λ* stereochemistry; both cage enantiomers are present in the crystal. The anthracene units lie tangent to the edges of the tetrahedron, affording a cavity that is almost completely enclosed by the ligands, with pores of less than 1.4 Å in diameter. The Fe-Fe distances are in the range 16.906(1)-17.322(1) Å (average 17.1 Å) and the cavity volume was calculated to be 518 $Å^3$ (Figure S54).

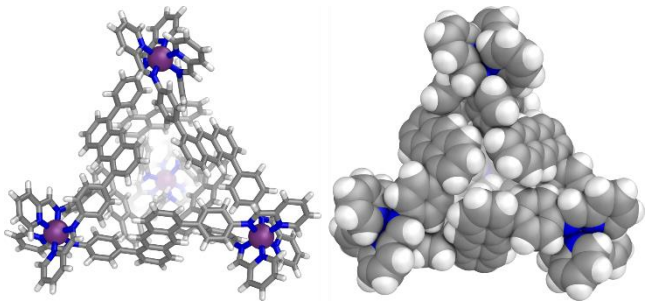

Figure 1. Two views of the cationic part of the crystal structure of **1**. Counterions and solvents are omitted for clarity.

We tested the Diels-Alder reactivity of cage **1** towards TCNE, which is known to undergo rapid donor-acceptor assisted[25] Diels-Alder cycloaddition with anthracene at room temperature.[26] The reaction between **1** and excess TCNE (8 equiv per anthracene) in CH_3CN resulted in the formation of modified cage **2** within 16 h at 298 K. The major set of peaks in the ESI-MS of the reaction mixture (Figure S12) corresponded to the $Fe^{II}_4L'_6$ cage (where L' is the TCNE Diels-Alder adduct of the original ligand L). The ^{1}H NMR spectrum of the resulting mixture was intractably complex, which we attribute to the presence of a mixture of low-symmetry diastereomeric products that arise from Diels-Alder reactions occurring on both the interior and exterior faces of anthracene ligands (Figure S11). The dynamic nature of the system precluded isolation of individual species from this mixture.

Despite the difficulty of performing meaningful NMR analysis on this mixture of diastereomers, we investigated the ability of cage **2** to act as a host. Fullerene C_{60} was identified as a potential guest for both **1** and **2** due to a predicted size and shape match with the large internal cavities of the cages and the potential for aromatic stacking with the walls of the cage. Excess C_{60} (5 equiv) was thus added to a CD_3CN solution of **2** and the suspension was stirred at 298 K for 4 days. ESI-MS confirmed formation of the 1:1 host-guest complex [C_{60} ⊂ **2**] with no peaks from the free host detected in the ESI mass spectrum (Figure S32). In contrast to **2**, the ^{1}H NMR spectrum of [C_{60} ⊂ **2**] showed a major product with a single set of ligand resonances, consistent with restoration of *T* point symmetry (Figure S25). The addition of C_{60} thus brought about a re-equilibration among the different diastereomers of **2**, likely via a deligation-religation process,[27] such that the *T*-diastereomer with all TCNE residues on the exterior of the cage predominated. We infer this diastereomer to maximize cavity size and thus binding affinity for this large guest. The success of the PAM reaction employed to synthesize **2** was verified by a shift in the ^{1}H resonance for the 9,10-anthracenyl protons from 8.16 ppm in **1** to 5.22 ppm in [C_{60} ⊂ **2**] and the appearance of corresponding new aliphatic ^{13}C NMR resonances at 49.7 and 47.0 ppm. The ^{13}C NMR spectrum also showed an intense peak at 141.8 ppm for C_{60}, despite its insolubility in CD_3CN,[28] providing further evidence for the encapsulation of C_{60} by **2**.

The structure of [C_{60} ⊂ **2**] was confirmed unambiguously by single-crystal X-ray analysis, showing successful PAM of all six cage ligands with TCNE and retention of overall *T*-symmetry (Figure 2). The Fe-Fe distances of 18.343(3)-18.362(3) Å (average 18.4 Å) are lengthened by an average of 1.3 Å relative to **1**. The increase in Fe-Fe separation in addition to the convex nature of the modified ligand results in an expanded cavity volume of 752 $Å^3$.

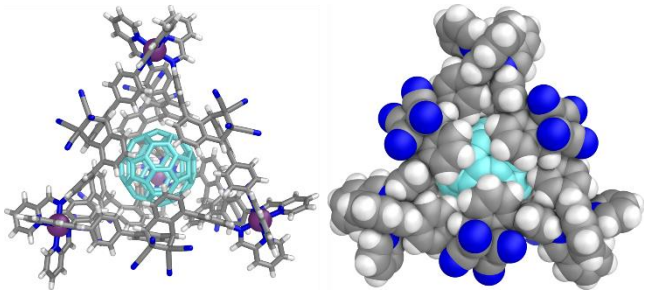

Figure 2. Two views of the cationic part of the crystal structure of [C_{60} ⊂ **2**]. Counterions, solvents and disorder are omitted for clarity.

In order to explore the scope of guest binding within **2**, the cage was also investigated as a host for the large anion $[Co(C_2B_9H_{11})_2]^-$. Addition of $Na[Co(C_2B_9H_{11})_2]$ (5 equiv) to **2** in CD_3CN resulted in formation of a new species with a similar diffusion coefficient to [C_{60} ⊂ **2**] but with four signals per ligand environment in the ^{1}H NMR spectrum, suggesting a C_3-symmetric host framework.[29] ESI-MS confirmed that the cage remained intact. We infer that $[Co(C_2B_9H_{11})_2]^-$ is encapsulated by **2** as anion metathesis would not be expected to induce diastereomeric reconfiguration. The bound $[Co(C_2B_9H_{11})_2]^-$ was displaced by C_{60} at 323 K (Figure S40) indicating that **2** has a higher affinity for the fullerene guest, which we infer to result from a better size and shape match between the host cavity and the spherical guest.

In order to probe the effect of PAM on guest binding, we also investigated precursor cage **1** as a host for $[Co(C_2B_9H_{11})_2]^-$ and

C_{60}. No encapsulation was observed by NMR following addition of $Na[Co(C_2B_9H_{11})_2]$ (5 equiv) to **1** in CD_3CN. Binding of $[Co(C_2B_9H_{11})_2]^-$ within **2** but not **1** thus demonstrates the utility of PAM as a means to tailor the host-guest properties of a metal-organic cage.

The reaction between **1** and excess C_{60} (5 equiv) in CD_3CN yielded a new product with a well-resolved but complex ^1H NMR spectrum. All peaks between 4.04 and 9.16 ppm displayed a single diffusion constant, nearly identical to that observed for **1**, in the diffusion ordered ^1H NMR (DOSY) spectrum (Figure S22), suggesting that they belonged to a single species of similar size to the original cage. One-dimensional pure shift (PSYCHE)[30] and two-dimensional NMR spectroscopy allowed the assignment of the major peaks to four magnetically distinct environments of equal intensity per ligand proton, consistent with the formation of a product of C_3 symmetry. ESI-MS results were consistent with a 1:1 adduct [C_{60} • **1**].

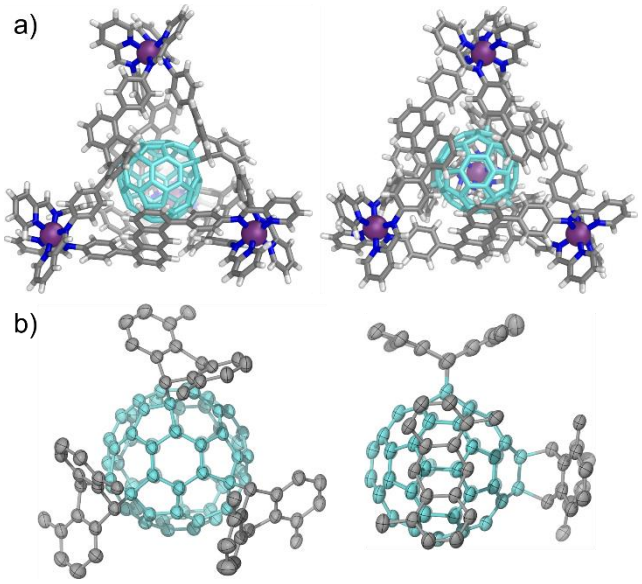

Figure 3. (a) Two views of the cationic part of the crystal structure of [C_{60} • **1**]. (b) Cutout of the tris(anthracenyl)C_{60} portion. Counterions and solvents are omitted for clarity.

The solid-state structure of [C_{60} • **1**] was elucidated by single-crystal X-ray analysis. The crystal structure revealed a covalent Diels-Alder adduct between **1** and C_{60} (Figure 3), where the encapsulated C_{60} had undergone cycloaddition with three anthracene ligands that share an apical vertex of the cage. As is usual with C_{60} functionalization, exclusively the double bonds between two six-membered rings had reacted. With respect to the first position of reaction, the second position was on the same equator (*e*) of the fullerene rather than on the same hemisphere (*cis*) or on the opposite hemisphere (*trans*).[31] The same regiochemical relationship exists between all three functionalization sites giving an overall orthogonal (*e*,*e*,*e*)-trisadduct. The newly formed long C-C bonds are in the range 1.57(1)-1.61(1) Å, similar to those reported for a related adduct.[32] The three modified ligands each link the apical iron(II) center with one of the three basal iron(II) centers (Fe···Fe distances 17.678(2)-18.086(3) Å) while three unmodified basal ligands bridge pairs of iron(II) centers around the bottom face of the tetrahedron with slightly shorter Fe···Fe distances of 17.156(2)-17.307(3) Å. In contrast to homochiral **1**, the handedness of the apical Fe^{II} center of [C_{60} • **1**] is opposite to those of the basal iron(II) centers; both *ΛΛΛΛ* and *ΔΔΔΔ* enantiomers are present in the unit cell. The assembly thus possesses overall non-crystallographic C_3 symmetry with a threefold symmetry axis passing through the center of the basal face (Figure 3). Despite reaction of the C_{60} with ligands that define one vertex of the cage, the fullerene is located almost exactly at the center of the Fe_4 tetrahedron. The presence of attractive aromatic interactions between the fullerene and the unreacted anthracenes may be stabilizing C_{60} in this more central position.

The functionalization of fullerenes often leads to multiple products due to different numbers of functionalization events occurring and different regio- and stereoisomers forming.[33] Obtaining selectivity for a single adduct is highly challenging and often requires permanent covalent tethering between reactants.[34] The orthogonal (*e*,*e*,*e*)-trisadduct of C_{60} is rare,[32] and this adduct with anthracene units has been reported to be thermally unstable at room temperature.[32] Solutions of [C_{60} • **1**] were stable at 323 K for several days but decomposition was observed at 343 K. The (*e*,*e*,*e*)-trisadduct is chiral, and it is notable that the stereochemistry of the adduct is determined by the chirality of the cage framework with complete diastereoselectivity.

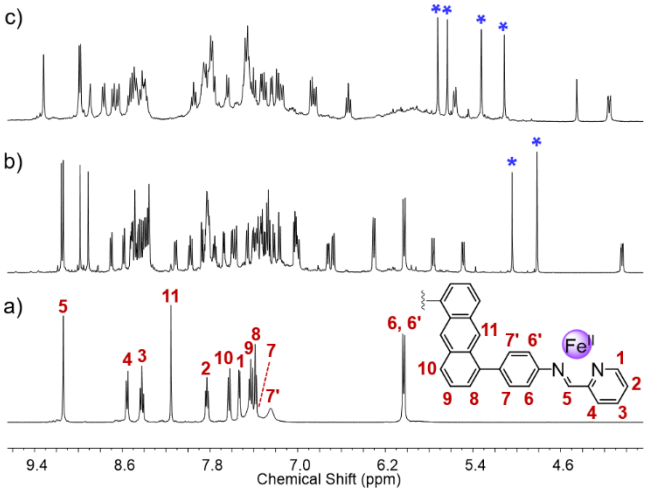

Figure 4. Partial ^1H NMR spectra (500 Hz, CD_3CN, 298 K) of (a) *T*-symmetric cage **1** (b) C_3-symmetric [C_{60} • **1**] and (c) C_3-symmetric [C_{60} • **3**]. The 9,10-dihydroanthracenyl protons of [C_{60} • **1**] and [C_{60} • **3**] are marked with blue asterisks.

The solution NMR data for [C_{60} • **1**] are consistent with the solid state structure (Figure 4), with the basal metal centers giving rise to three magnetically distinct environments and the apical metal center giving rise to one environment. Remarkably, NMR integration indicated the reaction of **1** with C_{60} to be more than 95% selective for the formation of *tris*-adduct [C_{60} • **1**], despite the presence of six anthracene panels and the potential for multiple adducts involving up to six cycloadditions and multiple regio- and stereoisomers of some adducts.

Noting that adduct [C_{60} • **1**] still contained three unmodified anthracene moieties, we sought to carry out further PAM through reaction of the remaining anthracene groups with TCNE. The reaction of [C_{60} • **1**] with excess TCNE (5 equiv per anthracene) in CD_3CN at 298 K was followed by ^1H NMR. Peaks corresponding to [C_{60} • **1**] were observed to disappear with appearance of a new set of peaks having the same overall number of signals, indicating that the C_3 symmetry of the assembly was maintained in the new product (Figure 4). The presence of four singlets in the range 5.1-5.7 ppm is consistent with complete PAM of the remaining ligands. ESI-MS confirmed formation of mixed ligand adduct [C_{60} • **3**], where the three basal ligands in [C_{60} • **1**] had undergone cycloaddition with TCNE (Figure 5).

We have shown that anthracene-edged tetrahedral cage **1** can undergo Diels-Alder cycloadditions both with the electron-deficient dienophile TCNE and with the fullerene C_{60}. Two singular adducts can be obtained depending on the order of reaction

with TCNE and C_{60} (Scheme 2). Treatment with TCNE followed by C_{60} gave rise to host-guest complex [$C_{60} \subset$ **2**], where C_{60} is non-covalently encapsulated inside a TCNE modified cage with bent dihydroanthracene panels. Reversing the order of reactant addition led to the formation of [C_{60} • **3**], where three of the ligands have undergone cycloaddition with C_{60} and the other three have reacted with TCNE, representing an unusual route to mixed-ligand complexes. Addition of an excess of both TCNE and C_{60} concurrently also afforded [$C_{60} \subset$ **2**] due to the greater rate of reaction between the anthracene panels and TCNE.

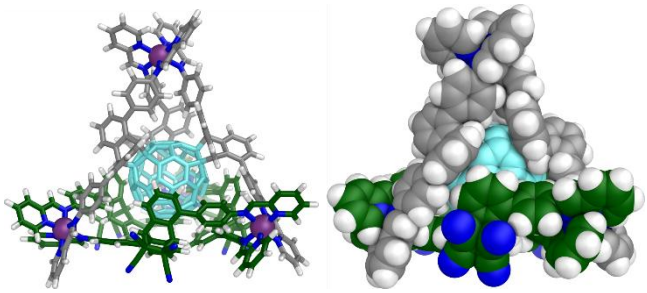

Figure 5. Two views of the MM3-optimized molecular model of [C_{60} • **3**], based on the single crystal X-ray structure of [C_{60} • **1**]. The TCNE-modified ligands are colored green.

Although the insolubility of C_{60} in acetonitrile precluded us from quantifying the affinity of **1** or **3** for this guest, we infer the six C–C bonds formed during binding to imply a very high affinity. Future work will seek to adapt the methodology presented here to obtain functionalized fullerene derivatives that would be difficult to obtain selectively by other means.

ASSOCIATED CONTENT

Supporting Information

The Supporting Information is available free of charge on the ACS Publications website at DOI:

X-ray data for **1** (CCDC 1486377) (CIF).

X-ray data for [C_{60} • **1**] (CCDC 1486378) (CIF).

X-ray data for [$C_{60} \subset$ **2**] (CCDC 1486379) (CIF).

Synthetic details, characterization data, NMR and mass spectra (PDF).

AUTHOR INFORMATION

Corresponding Author

*jrn34@cam.ac.uk.

Notes

The authors declare no competing financial interests.

ACKNOWLEDGMENT

This work was supported by the UK Engineering and Physical Sciences Research Council (EPSRC). We thank the EPSRC Mass Spectrometry Service at Swansea for carrying out the high resolution mass spectrometry. B.S.P. acknowledges the Herchel Smith Research Fellowship from the University of Cambridge and the Fellowship from Corpus Christi College, Cambridge. We also thank Derrick A. Roberts and the NMR service team at the Department of Chemistry, University of Cambridge for performing some NMR experiments.

REFERENCES

(1) (a) Schneider, M. W.; Oppel, I. M.; Griffin, A.; Mastalerz, M. *Angew. Chem. Int. Ed.* **2013**, *52*, 3611; (b) Brega, V.; Zeller, M.; He, Y.; Peter Lu, H.; Klosterman, J. K. *Chem. Commun.* **2015**, *51*, 5077.

(2) Zhao, D.; Tan, S.; Yuan, D.; Lu, W.; Rezenom, Y. H.; Jiang, H.; Wang, L.-Q.; Zhou, H.-C. *Adv. Mater.* **2011**, *23*, 90.

(3) Roberts, D. A.; Castilla, A. M.; Ronson, T. K.; Nitschke, J. R. *J. Am. Chem. Soc.* **2014**, *136*, 8201.

(4) Beves, J. E.; Danon, J. J.; Leigh, D. A.; Lemonnier, J.-F.; Vitorica-Yrezabal, I. J. *Angew. Chem. Int. Ed.* **2015**, *54*, 7555.

(5) Zheng, W.; Chen, L.-J.; Yang, G.; Sun, B.; Wang, X.; Jiang, B.; Yin, G.-Q.; Zhang, L.; Li, X.; Liu, M.; Chen, G.; Yang, H.-B. *J. Am. Chem. Soc.* **2016**, *138*, 4927.

(6) (a) Fuller, A.-M.; Leigh, D. A.; Lusby, P. J.; Oswald, I. D. H.; Parsons, S.; Walker, D. B. *Angew. Chem. Int. Ed.* **2004**, *43*, 3914; (b) Kaucher, M. S.; Harrell, W. A.; Davis, J. T. *J. Am. Chem. Soc.* **2005**, *128*, 38; (c) Fuller, A.-M. L.; Leigh, D. A.; Lusby, P. J.; Slawin, A. M. Z.; Walker, D. B. *J. Am. Chem. Soc.* **2005**, *127*, 12612; (d) Leigh, D. A.; Lusby, P. J.; McBurney, R. T.; Morelli, A.; Slawin, A. M. Z.; Thomson, A. R.; Walker, D. B. *J. Am. Chem. Soc.* **2009**, *131*, 3762.

(7) (a) Chakrabarty, R.; Stang, P. J. *J. Am. Chem. Soc.* **2012**, *134*, 14738; (b) Barran, P. E.; Cole, H. L.; Goldup, S. M.; Leigh, D. A.; McGonigal, P. R.; Symes, M. D.; Wu, J.; Zengerle, M. *Angew. Chem. Int. Ed.* **2011**, *50*, 12280; (c) Han, S.; Ma, Z.; Hopson, R.; Wei, Y.; Budil, D.; Gulla, S.; Moulton, B. *Inorg. Chem. Commun.* **2012**, *15*, 78.

(8) Acharyya, K.; Mukherjee, P. S. *Chem. Eur. J.* **2015**, *21*, 6823.

(9) Wang, M.; Lan, W.-J.; Zheng, Y.-R.; Cook, T. R.; White, H. S.; Stang, P. J. *J. Am. Chem. Soc.* **2011**, *133*, 10752.

(10) Roberts, D. A.; Pilgrim, B. S.; Cooper, J. D.; Ronson, T. K.; Zarra, S.; Nitschke, J. R. *J. Am. Chem. Soc.* **2015**, *137*, 10068.

(11) Samanta, D.; Chowdhury, A.; Mukherjee, P. S. *Inorg. Chem.* **2016**, *55*, 1562.

(12) Young, M. C.; Johnson, A. M.; Hooley, R. J. *Chem. Commun.* **2014**, *50*, 1378.

(13) Tanabe, K. K.; Cohen, S. M. *Chem. Soc. Rev.* **2011**, *40*, 498.

(14) Cook, T. R.; Stang, P. J. *Chem. Rev.* **2015**, *115*, 7001.

(15) Custelcean, R.; Bonnesen, P. V.; Duncan, N. C.; Zhang, X.; Watson, L. A.; Van Berkel, G.; Parson, W. B.; Hay, B. P. *J. Am. Chem. Soc.* **2012**, *134*, 8525.

(16) Cullen, W.; Misuraca, M. C.; Hunter, C. A.; Williams, N. H.; Ward, M. D. *Nat. Chem.* **2016**, *8*, 231.

(17) Cook, T. R.; Vajpayee, V.; Lee, M. H.; Stang, P. J.; Chi, K.-W. *Acc. Chem. Res.* **2013**, *46*, 2464.

(18) Yoshizawa, M.; Klosterman, J. K. *Chem. Soc. Rev.* **2014**, *43*, 1885.

(19) (a) Kishi, N.; Li, Z.; Yoza, K.; Akita, M.; Yoshizawa, M. *J. Am. Chem. Soc.* **2011**, *133*, 11438; (b) Ramsay, W. J.; Szczypiński, F. T.; Weissman, H.; Ronson, T. K.; Smulders, M. M. J.; Rybtchinski, B.; Nitschke, J. R. *Angew. Chem. Int. Ed.* **2015**, *54*, 5636.

(20) Atherton, J. C. C.; Jones, S. *Tetrahedron* **2003**, *59*, 9039.

(21) Masci, B.; Pasquale, S.; Thuéry, P. *Org. Lett.* **2008**, *10*, 4835.

(22) Li, P.; Wong, B. M.; Zakharov, L. N.; Jasti, R. *Org. Lett.* **2016**, *18*, 1574.

(23) Miyaura, N.; Suzuki, A. *Chem. Rev.* **1995**, *95*, 2457.

(24) (a) Ronson, T. K.; Zarra, S.; Black, S. P.; Nitschke, J. R. *Chem. Commun.* **2013**, *49*, 2476; (b) Lewing, D.; Koppetz, H.; Hahn, F. E. *Inorg. Chem.* **2015**, *54*, 7653; (c) Frischmann, P. D.; Kunz, V.; Stepanenko, V.; Würthner, F. *Chem. Eur. J.* **2015**, *21*, 2766; (d) Campbell, V. E.; Guillot, R.; Riviere, E.; Brun, P.-T.; Wernsdorfer, W.; Mallah, T. *Inorg. Chem* **2013**, *52*, 5194; (e) Yi, S.; Brega, V.; Captain, B.; Kaifer, A. E. *Chem. Commun.* **2012**, *48*, 10295; (f) Wu, Y.; Zhou, X.-P.; Yang, J.-R.; Li, D. *Chem. Commun.* **2013**, *49*, 3413; (g) Sham, K.-C.; Yiu, S.-M.; Kwong, H.-L. *Inorg. Chem.* **2013**, *52*, 5648.

(25) Wise, K. E.; Wheeler, R. A. *J. Phys. Chem. A* **1999**, *103*, 8279.

(26) (a) Lotfi, M.; Roberts, R. M. G. *Tetrahedron* **1979**, *35*, 2131; (b) Handoo, K. L.; Lu, Y.; Parker, V. D. *J. Am. Chem. Soc.* **2003**, *125*, 9381.

(27) Clegg, J. K.; Cremers, J.; Hogben, A. J.; Breiner, B.; Smulders, M. M. J.; Thoburn, J. D.; Nitschke, J. R. *Chem. Sci.* **2013**, *4*, 68.

(28) Semenov, K. N.; Charykov, N. A.; Keskinov, V. A.; Piartman, A. K.; Blokhin, A. A.; Kopyrin, A. A. *J. Chem. Eng. Data* **2009**, *55*, 13.

(29) Meng, W.; Clegg, J. K.; Thoburn, J. D.; Nitschke, J. R. *J. Am. Chem. Soc.* **2011**, *133*, 13652.

(30) Foroozandeh, M.; Adams, R. W.; Meharry, N. J.; Jeannerat, D.; Nilsson, M.; Morris, G. A. *Angew. Chem. Int. Ed.* **2014**, *53*, 6990.

(31) Hirsch, A.; Lamparth, I.; Karfunkel, H. R. *Angew. Chem. Int. Ed.* **1994**, *33*, 437.

(32) Duarte-Ruiz, A.; Wurst, K.; Kräutler, B. *Helv. Chim. Acta* **2008**, *91*, 1401.

(33) Qian, W.; Rubin, Y. *Angew. Chem. Int. Ed.* **2000**, *39*, 3133.

(34) Taki, M.; Sugita, S.; Nakamura, Y.; Kasashima, E.; Yashima, E.; Okamoto, Y.; Nishimura, J. *J. Am. Chem. Soc.* **1997**, *119*, 926.

Insert Table of Contents artwork here